Synoptic- and Frontal-Scale Influences on Tropical Transition Events in the Atlantic Basin. Part I: A Six-Case Survey

ANDREW L. HULME AND JONATHAN E. MARTIN

Department of Atmospheric and Oceanic Sciences, University of Wisconsin—Madison, Madison, Wisconsin

ABSTRACT

The process by which a baroclinic, vertically sheared, extratropical cyclone is transformed into a warm-core, vertically stacked tropical cyclone is known as tropical transition. Six recent tropical transitions of strong extratropical precursors in the subtropical North Atlantic are compared to better understand the manner by which some of the canonical structures and dynamical processes of extratropical cyclones serve to precondition the cyclone for transition. All six transitions resulted from the interaction between a surface baroclinic zone and an upper-level trough. During the extratropical cyclogenesis of each storm, a period of intense near-surface frontogenesis along a bent-back warm front occurred to the northwest of each sea level pressure minimum. Within the resultant circulation, diabatic redistribution of potential vorticity (PV) promoted the growth of a low-level PV maximum near the western end of the warm front. Concurrently, the upper-level PV anomaly associated with each trough was deformed into the treble clef structure characteristic of extratropical occlusion. Thus, by the end of the transitioning process and just prior to its becoming fully tropical, each cyclone was directly beneath a weakened upper-level trough in a column with weak vertical shear and weak thermal contrasts. The presence of convection to the west and southwest of the surface cyclone at the time of frontogenesis and upper-level PV deformation suggests that diabatic heating contributes significantly to the process of tropical transition in a manner that is consistent with its role in extratropical occlusion. Thus, it is suggested that tropical transition is encouraged whenever extratropical occlusion occurs over a sufficiently warm ocean surface.

1. Introduction

Cyclonic storms are usually classified as either tropical or extratropical based upon their geographic location and their appearance in satellite imagery, which testify to the different structures, energetics, and dynamics that characterize the two types. Mature tropical cyclones are axisymmetric in appearance, possess a tropospheric-deep warm inner core, display their strongest circulations near the surface, and derive energy from air–sea interaction. Extratropical cyclones are usually asymmetric in both the temperature and cloud fields (i.e., the comma-shaped cloud canopy), and their circulations increase in intensity with height and are driven by baroclinic energy conversion.

Despite the conceptual appeal of such well-defined categories, nature is not so binary since actual cyclones not only frequently exhibit properties of both types but also share important developmental mechanisms. For instance, extratropical marine cyclones can develop eye-like features and warm-core centers (e.g., Bosart 1981; Reed and Albright 1986) while hurricane-like structures and convectively driven vortices can result from the passage of mesoscale disturbances over the relatively warm water of the Mediterranean Sea (Reale and Atlas 2001) or even the Great Lakes (Sousounis et al. 2001). Polar lows have been observed with small-scale warm cores (e.g., Rasmussen 1981; Moore and Vonder Haar 2003) and are at least partially driven by diabatic processes (Montgomery and Farrell 1992). Usually considered detrimental to tropical cyclogenesis, moderate amounts of vertical shear have been shown to contribute to the early development of tropical depressions (Bracken and Bosart 2000; Molinari et al. 2004). Upper-level troughs can strongly influence tropical cyclone development as the interaction between a mature tropical

Corresponding author address: Jonathan E. Martin, Department of Atmospheric and Oceanic Sciences, University of Wisconsin—Madison, 1225 W. Dayton St., Madison, WI 53705.
E-mail: jemarti1@wisc.edu

cyclone and an upstream trough in certain synoptic settings can lead to deepening (Hanley et al. 2001). Clearly, no sharp boundary between the two cyclone types exists; a realization that led Hart (2003) to consider the concept of a cyclone phase space in which the full "spectrum" of cyclones may be classified based upon the physical properties of thermal symmetry and variation of intensity with height.

The notion of a spectrum of cyclonic disturbances is perhaps most interesting when considering a storm that changes classifications during its life cycle as such a change suggests companion changes in dynamics and energetics. Several recent studies (e.g., Foley and Hanstrum 1994; Harr and Elsberry 2000; Klein et al. 2000; Ritchie and Elsberry 2001; Hart and Evans 2001; Sinclair 2002; Jones et al. 2003; Hart et al. 2006) have examined a process known as extratropical transition (ET) in which a tropical cyclone recurves to the midlatitudes, interacts with the indigenous baroclinicity, acquires frontal structure and becomes fully extratropical. The inverse of ET is tropical transition (TT), in which a nontropical, frontal, baroclinic disturbance, often of midlatitude origin, develops and transforms into a tropical cyclone. Tropical transitions tend to occur in the subtropical ocean (poleward of 20° latitude) where midlatitude weather systems can ingest considerable moisture from the warm underlying ocean (Davis and Bosart 2003, 2004). While storms that undergo tropical transition rarely reach major hurricane status, they can be associated with hazardous sensible weather (Beven et al. 2003) and, as a consequence of their formation at high latitude, are also likely to affect land that is rarely hit by hurricanes [e.g. Hurricane Juan in 2003; McTaggart-Cowan et al. (2006)]. Recent work by McTaggart-Cowan et al. (2008) suggests that such tropical transition events represent ~28% of all tropical cyclones in the Atlantic basin.[1]

Davis and Bosart (2003) surveyed 10 cases of tropical transition that occurred in the 2000 and 2001 Atlantic hurricane seasons. They found that each of these cyclones had initial 900–200-hPa vertical shear values near or above the empirical threshold at which tropical cyclogenesis is unlikely.[2] However, for each transitioning storm, vertical shear decreased below the critical value by the time each cyclone became tropical. Therefore, identifying the process or processes by which the cyclone sheds its initially highly sheared environment is funda-

mental to understanding tropical transition. One obvious process, operating in the extratropical cyclone life cycle, which results in reduced vertical shear above the surface cyclone center is the midlatitude occlusion process in which the originally asymmetric thermal structure is rendered equivalent barotropic with an attendant decrease in vertical shear above the sea level pressure minimum (Palmén and Newton 1969). Indeed, Davis and Bosart (2003, 2004) recognize the importance of extratropical occlusion in the tropical transition process.[3]

Posselt and Martin (2004) examined the effect of latent heat release on the development of the occluded thermal structure in a robust winter storm by comparing companion full physics (FP) and no-latent-heat-release (NLHR) simulations of the event performed using the fifth-generation Pennsylvania State University–National Center for Atmospheric Research (PSU–NCAR) Mesoscale Model version 3.5 (MM5). Concentrating on the role of latent heat release on the evolution of the upper-tropospheric potential vorticity (PV) morphology, they showed that direct destruction of upper-tropospheric PV by midtropospheric latent heat release initiated formation of a local, upper-tropospheric PV minimum to the northwest of the surface cyclone. The production of this PV minimum initiated a cutting off of the upper-tropospheric PV anomaly associated with the surface development. The upper-tropospheric circulation associated with the cutoff anomaly, in turn, advected low values of PV into the developing PV trough. This combination of kinematic and diabatic processes produced both the tropopause PV treble clef (Martin 1998) as well as the underlying warm occluded thermal structure in the FP simulation. Though an adiabatic kinematic tendency to produce a PV treble clef operated in the NLHR simulation, the resulting PV and thermal structures were weaker and slower to evolve than those produced in the FP simulation. They therefore concluded that latent heat release plays a fundamental role in the midlatitude occlusion process.

In their model-aided analysis of a tropical transition event (Hurricane Michael in 2000), Davis and Bosart (2003) found that strong latent heating, organized in the convection associated with the baroclinic precursor, removed vertical shear by redistributing PV in the vertical (Raymond 1992). In addition, the outflow from the convection helped to horizontally displace large PV gradients away from the column directly above the surface cyclone creating a low-shear environment in

---

[1] More specifically, McTaggart-Cowan et al. (2008) found that 13% (15%) of all tropical cyclones arose from tropical transition events involving a weak (strong) precursor.

[2] Generally, unless the vertical shear in the 200–900-hPa layer (i.e., from the tropopause to the boundary layer) is less than 10–15 m s^{-1}, tropical cyclogenesis is unlikely (e.g., DeMaria et al. 2001).

[3] Davis and Bosart (2004) state, as a forecast rule for SEC transition events, that "the precursor cyclone must occlude and remain over warm water (> ~26°C) for at least a day following occlusion."

which a warm-core tropical cyclone could be nurtured. An analysis of additional cases by Davis and Bosart (2004) suggested that convection upshear of the precursor cyclone may be particularly efficient at horizontally displacing large PV gradients, especially when the baroclinic precursor is exceptionally strong.[4]

Focusing on the apparent ubiquity of upshear[5] convection in the tropical transition of SECs, the goal of the present work is to examine the role that the frontal structure and frontal dynamics of the precursor disturbance have on focusing moist ascent and the resulting deep convection. The paper will present a survey of six different cases of tropical transition (each characterized by a strong baroclinic precursor) that occurred in the subtropical Atlantic between 2000 and 2005. The analysis suggests that a dynamic–diabatic feedback between lower-tropospheric frontogenesis, and the extratropical occlusion process (which involves upshear convection and associated diabatic PV redistribution), is essential to the process of tropical transition. In a companion paper (Hulme and Martin 2009), we choose a particular case, Atlantic Hurricane Karen in 2001, and perform a numerical simulation of it using the Weather Research and Forecasting (WRF) model to further refine understanding of the mesoscale structures, physical processes, and associated-scale interactions associated with tropical transition. The present paper is organized in the following manner. Section 2 describes the dataset and methodology used in this analysis. It also describes the relationship between PV and diabatic heating as well as upper-level PV gradients and vertical shear that provides useful background for understanding elements of the tropical transition process. In section 3 a cursory overview of six different cases of tropical transition that occurred in the subtropical Atlantic Ocean between 2000 and 2005 is presented. An analysis of the distribution of low-level frontogenesis, upper- and lower-level PV and their diabatically forced tendencies, as well as upshear convection in the chosen cases of tropical transition is offered in section 4. The goal here is not to provide modest case studies of each event but rather to highlight the similarities between the cases. Section 5 summarizes the results, discusses them in the context of prior work, and suggests future directions for the study of tropical transitions.

---

[4] Tropical transition involving strong extratropical cyclone (SEC) precursors were identified by Davis and Bosart (2004) as events in which a robust extratropical cyclone precedes the transtion.

[5] The term "upshear" means to the west or southwest of the surface cyclone.

2. Background and case overviews

Tropical transition is the process by which a baroclinic, vertically sheared extratropical cyclone is transformed into a warm core, weakly sheared, vertically stacked tropical cyclone. Given TT's dependence on vertical shear reduction, it is useful to consider some mechanisms, operating in the context of the extratropical cyclone life cycle, whereby the vertical shear can be reduced.

a. Shear reduction

The occlusion process itself, wherein the cyclone adopts an equivalent barotropic structure and the vertical shear above the sea level pressure minimum is greatly reduced (Palmén and Newton 1969), represents perhaps the most obvious shear reduction mechanism in the canonical extratropical cyclone life cycle. Martin (1998) showed that adoption of a "treble clef" shape to the tropopause-level PV distribution was a sufficient condition for asserting the presence of an occluded thermal structure in the underlying troposphere.

Shear reduction mechanisms can also be understood by examining the relationship between upper-level PV gradients and vertical shear. From the quasigeostrophic perspective, PV and geopotential are related via an elliptic, linear operator Λ. Specifically,

$$q = \frac{1}{f_o}\nabla^2\phi + \frac{f_o}{\sigma}\frac{\partial^2\phi}{\partial p^2} + f = \Lambda(\phi) + f, \qquad (1)$$

where q is quasigeostrophic PV, ϕ is geopotential, f is the Coriolis term, and f_o and σ are constant Coriolis and stratification typical of the midlatitudes, respectively. Taking the spatial derivative of (1), ignoring variations in f, and assuming geostrophy, an expression equating the upper-level winds to the PV gradient can be found,

$$\frac{\partial q}{\partial x} = \Lambda(f_o v_g), \quad \frac{\partial q}{\partial y} = \Lambda(-f_o u_g), \qquad (2)$$

where u_g and v_g are components of the geostrophic wind. Given the ellipicity of Λ, in the Northern Hemisphere a local maximum (minimum) in the gradient of q would be correlated with a minimum (maximum) in meridional wind and a maximum (minimum) in zonal wind. In most cases, areas of zero PV gradient are areas of light upper-level winds. Ignoring near-surface winds, the largest values of vertical shear will then be collocated with the largest magnitudes of upper-level PV gradient (Hoskins et al. 1985; Davis and Bosart 2003).

Potential vorticity can be redistributed vertically by introducing a differential diabatic heat source [e.g., latent heat release (LHR)] into the column. From Hoskins

TABLE 1. Parameters of interest for each of the selected cases of tropical transition. The Time of tropical designation was determined using cyclone phase space diagnostics developed by Hart (2003). SLP and wind data are taken from HURDAT data.

Storm	Dates	Time of tropical designation	Min SLP at TD (hPa)	Min SLP overall (hPa)	Max winds (kt)
Michael	15–20 Oct 2000	1200 UTC 15 Oct	1003	965	85
Karen	11–15 Oct 2001	1200 UTC 12 Oct	988	982	70
Noel	4–6 Nov 2001	1200 UTC 3 Nov	986	986	65
Olga	23 Nov–4 Dec 2001	0000 UTC 24 Nov	989	973	80
Delta	19–29 Nov 2005	1200 UTC 22 Nov	983	980	60
Epsilon	29 Nov–9 Dec 2005	0600 UTC 29 Nov	993	981	75

et al. (1985), the Lagrangian PV tendency due to a diabatic heat source is represented by

$$\rho \frac{dP}{dt} = \boldsymbol{\eta}_a \cdot \nabla \dot{\theta}, \qquad (3)$$

where ρ is the atmospheric density, P is the potential vorticity, $\boldsymbol{\eta}_a$ is the three-dimensional absolute vorticity vector, and $\dot{\theta}$ is the diabatic heating rate (i.e., $d\theta/dt$). Assuming that the diabatic heating maximum is in the midtroposphere and the absolute vorticity vector is nearly vertical, PV will tend to increase (decrease) in the layer below (above) the heating maximum (Raymond 1992). The end result will be anomalously high PV in the lower troposphere, with lower values near the tropopause. Thus, a PV perspective suggests that shear can hypothetically be decreased over a cyclone by two methods: 1) decreasing the magnitude of the upper-level PV gradient through a diabatic process that homogenizes the PV field, or 2) either moving the surface cyclone (or reforming it) under tropospheric columns capped by weak PV gradients.

b. Data

The six-case survey presented here utilizes the 6-hourly Global Final Analysis (FNL) dataset provided by the National Centers for Environmental Prediction (NCEP). Standard meteorological variables were sampled at 50-hPa intervals from 1000 to 100 hPa on a 1° by 1° latitude–longitude grid. The Hurricane Best Track (HURDAT) database compiled by the Tropical Prediction Center (TPC) was utilized to determine the location and strength of each surface cyclone. However, since the cyclones studied here had often existed as extratropical cyclones for several days before being included in HURDAT, supplemental surface cyclone positions were determined from the FNL data. The time of tropical designation for each storm was defined as the time at which it was first analyzed as "warm core/symmetric" according to the cyclone phase space diagnostics of Hart (2003). (For all the storms except Epsilon,

we employed the cyclone phase space charts available online at http://moe.met.fsu.edu/cyclonephase/.)[6]

c. Case overviews

We next compare the evolutions of six cases of tropical transition involving strong extratropical cyclones (SECs). Sea level pressure (SLP) data taken from HURDAT along with the time of tropical designation as determined by cyclone phase space diagnostics are listed for each cyclone in Table 1. The tracks of the six storms are shown in Fig. 1.

Michael formed 750 km southwest of Bermuda on 14 October 2000 as a result of the interaction between an upper-level trough and a stationary front (Franklin et al. 2001). While becoming tropical on 15 October, the storm moved to the west and became stationary. Michael briefly reached category 2 strength just east of Nova Scotia late in the day on 19 October while transitioning into an intense extratropical cyclone.

On 10 October 2001, Karen formed downstream of an upper-level trough along a stationary front 1000 km south of Bermuda. The storm made a northwestward jog and passed very close to Bermuda while becoming tropical on 12 October. Karen became a hurricane for a short time on 14 October prior to making landfall in Nova Scotia on 15 October.

Noel resulted from a decaying, occluded cyclone in the north-central Atlantic that began to redevelop in response to the encroachment of an upper-level trough on 2 November 2001 (Beven et al. 2003). While extratropical, the storm moved quickly westward and then took a northward turn after becoming tropical on 3 November. Noel reached hurricane status on 5 November before undergoing an ET.

Olga originated from a persistent extratropical cyclone that by 22 November 2001 had moved 1000 km southeast of Bermuda. The storm moved eastward in the westerlies until 24 November when it became tropical

---

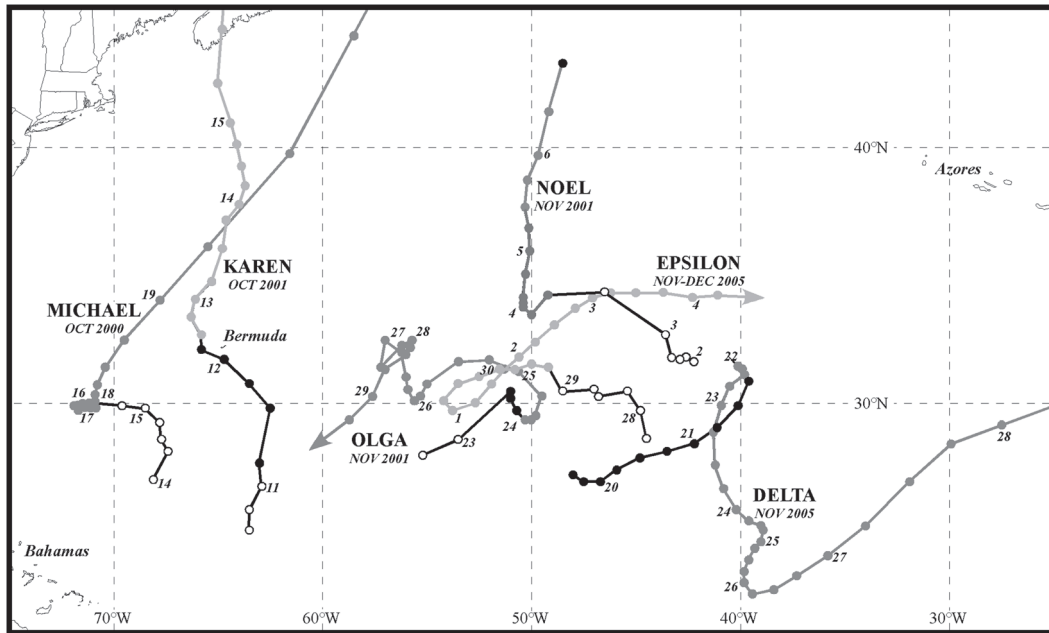[6] We used the FNL data to construct a similar cyclone phase space diagnostic for Epsilon.

FIG. 1. Cyclone tracks of each of the six tropical transition cases. Closed dots represent cyclone positions taken from HURDAT with open dots indicating supplemental cyclone positions taken from FNL analysis. Black lines/dots indicate positions at which the cyclone was considered nontropical (either extratropical or subtropical) and gray lines/dots indicates position at which the cyclone was considered tropical (note that different shades of gray have no significance except to demarcate different tracks). Number next to a dot indicates the 0000 UTC position for that date. Cyclone tracks lasting 5 days after tropical transition are truncated and end in an arrow.

and sat in the axis of a small-amplitude, negatively tilted, upper-level trough (Beven et al. 2003). By 25 November, the storm started moving westward. Olga was a hurricane from 26 to 28 November and did not dissipate until early December while near the Bahamas.

Delta began as an extratropical cyclone that formed on 19 November 2005 in the middle of the Atlantic. The system progressed eastward as an intensifying extratropical cyclone downwind of an upper-level trough until 1200 UTC 22 November when it became tropical and turned to the south-southwest. Delta's sustained winds reached a maximum intensity of 31 m s^{-1}, just below hurricane strength, on 25 November. After this, the system moved quickly eastward affecting the Canary Islands and Morocco on 29 November as a hybrid storm.

Epsilon developed on 28 November 2005 downstream of an upper-level trough along a stationary front 1800 km east of Bermuda. The cyclone moved westward while transitioning and became tropical on 29 November. Epsilon made a cyclonic loop before turning eastward on 1 December (Beven et al. 2008). Beginning on 3 December, Epsilon was a hurricane for 5 days with maximum winds up to 39 m s^{-1}. The system decayed on 9 December as a tropical depression.

Prior to transition, each storm either began to move westward with respect to its prior movement, deflected to

the west while moving northward (e.g., Michael), or experienced a decrease in forward speed while moving quickly eastward in the mean flow (e.g., Delta). In all cases except Michael, the precursors underwent a period of strengthening prior to tropical designation and attained sea level pressures of 993 hPa or below with surface winds in excess of 23 m s^{-1} before transition. After becoming tropical, most of the cyclones deepened only another 5–10 hPa; hence, a large fraction of the overall intensification of each storm occurred during its development as either an extratropical or subtropical cyclone.

The most apparent similarity in all six cases is that the precursor in each case resulted from the interaction of an upper-tropospheric trough with a low-level baroclinic zone beginning about three days prior to transition. The precursor to Michael developed along a southwest–northeast-oriented stationary front in the right entrance region of a jet on the eastern side of a large-amplitude upper-level trough (Fig. 2a). The precursor to Karen responded to a similar configuration except the upper-level jet was broader and the lower-level baroclinic zone was more zonally oriented (Fig. 2b). Noel developed in the left exit region of a zonal jet that was positioned south of 30°N at the base of a large-amplitude trough (Fig. 2c). As Noel's precursor was a robust cyclone several days before transition, the strongest baroclinicity had become
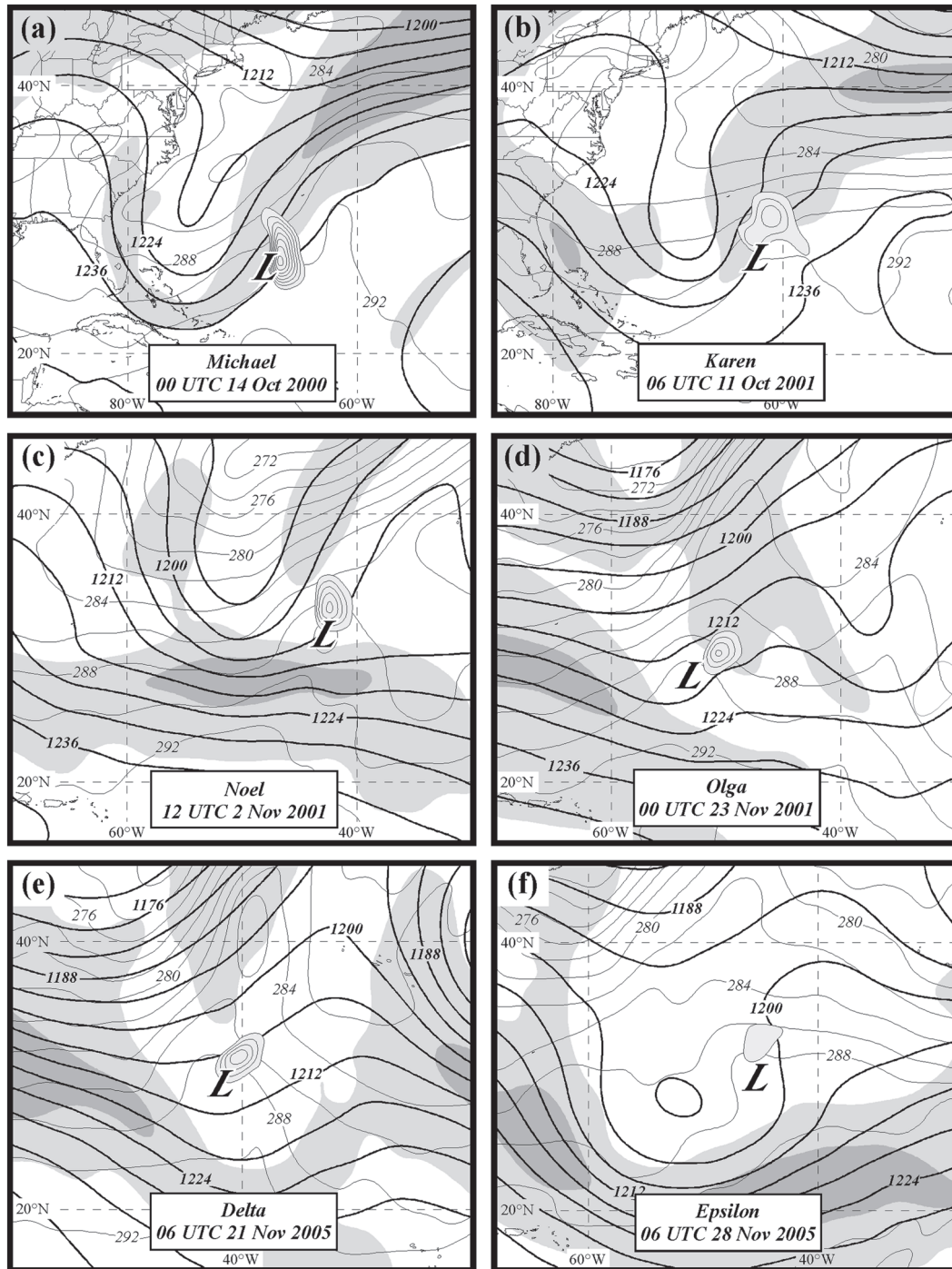
FIG. 2. FNL analyses of 200-hPa geopotential height, 900-hPa temperature, PVA by the thermal wind, and 200-hPa wind speed for (a) 0000 UTC 14 Oct 2000 (Michael), (b) 0600 UTC 11 Oct 2001 (Karen), (c) 1200 UTC 2 Nov 2001 (Noel), (d) 0000 UTC 23 Nov 2001 (Olga), (e) 0600 UTC 21 Nov 2005 (Delta), and (f) 0600 UTC 28 Nov 2005 (Epsilon). Thick black lines are geopotential height labeled in dam and contoured every 6 dam. Thin gray lines are 900-hPa temperature labeled in K and contoured every 2 K. Thin black lines (with shading) are regions of positive advection of 700-hPa geostrophic vorticity by the 500–900-hPa thermal wind, labeled in 10^{-9} m kg^{-1} and contoured every 2×10^{-9} m kg^{-1} starting at 2×10^{-9} m kg^{-1}. Shaded regions are 200-hPa wind speeds shaded every 20 m s^{-1} starting at 25 m s^{-1}. The "L" in (a)–(f) represents the position of the SLP minimum.

TABLE 2. Mean vertical shear (m s^{-1}) in the 200–900-hPa layer at 6-h intervals from 24 h before ($T - 24$) to 24 h after ($T + 24$) the time of tropical designation ($T = 0$) calculated using the FNL data. Shear is averaged over a 5° $\times$ 5° grid centered on the center of each storm in the analysis. The storm center was defined as the 900-hPa vorticity maximum averaged on a 3° $\times$ 3° grid.

	$T - 24$	$T - 18$	$T - 12$	$T - 6$	$T = 0$	$T + 6$	$T + 12$	$T + 18$	$T + 24$
Michael	32.6	31.9	30.3	27.1	18.4	15.2	12.5	12.1	10.7
Karen	30.7	29.6	19.1	15.1	7.4	11.9	12.0	11.8	11.6
Noel	20.6	18.9	15.7	15.6	12.9	11.5	13.5	11.5	12.4
Olga	14.6	19.1	16.8	12.4	12.4	10.5	7.9	8.5	11.8
Delta	19.8	17.1	14.9	17.1	14.2	11.4	10.2	15.4	18.0
Epsilon	16.2	9.7	10.4	10.8	7.5	11.0	10.6	11.1	9.6

positioned west of the SLP minimum at the time shown. The synoptic-scale settings in which Olga (Fig. 2d) and Delta (Fig. 2e) developed were similar to one another. In both cases, the precursor cyclone had existed for a few days as evidenced by the thermal ridge present in both low-level temperature fields. In addition, both cyclones became positioned near a small-amplitude trough axis in the left exit region of a northwesterly jet. Epsilon's precursor was more removed from an upper-level jet than the other five cases but was located downstream of an upper-level cutoff low (Fig. 2f). The baroclinicity in Epsilon extended along a warm front to the north and northeast of the SLP minimum. Located downshear of an upper-level trough, each cyclone was in a favorable area for deepening via vertical motions inferred from cyclonic vorticity advection by the thermal wind (Sutcliffe 1947; Trenberth 1978). Thus, even as proximate as one day or so before transitioning, each cyclone was ensconced in an environment supportive of extratropical deepening. During this period of baroclinic development, the vertical shear over each cyclone was at or above the 15 m s^{-1} threshold (Table 2) a result of each storm's proximity to an upper-level jet.

3. Synoptic settings of the six cases

a. Low-level frontogenesis

Prior idealized modeling work by Takayabu (1986), Xu (1990), and Schär and Wernli (1993) has suggested a relationship between lower-tropospheric frontogenesis along the warm front and the accumulation of vorticity (or PV) at the western end of the front. In their analysis of an isolated, adiabatic, semigeostrophic idealized cyclone, Schär and Wernli (1993) showed that westward, storm-relative, alongfront advection of vorticity, produced in association with frontogenesis and its attendant vertical circulation, accounted for the "stubbiness" of the warm frontal zone in the simulation. Additionally they showed that the alongfront vorticity advection resulted in a concentration of vorticity and baroclinicity at the western end of the frontal zone near the cyclone center.

A similar relationship between frontogenesis, its vertical circulation, and the lower-tropospheric potential

vorticity appears to characterize the cases under investigation here. Figure 3 displays the low-level (900 hPa) temperature, winds, frontogenesis, and (850–950-hPa layer) PV fields at the approximate time of maximum frontogenesis for each cyclone. At the time of tropical designation, Michael (Fig. 3a) had a well-defined warm front that wrapped around the SLP minimum as a bent-back front. Near the western end of the bent-back extension strong frontogenesis occurred to the northwest of Michael's robust PV maximum. Karen (Fig. 3b) was slightly less developed than Michael at the time shown, yet a strong linear band of frontogenesis existed along the cyclone's warm front and its bent-back extension. Just to the south of the most intense frontogenesis was an area of large, positive PV displaced slightly west of the SLP minimum. Noel (Fig. 3c) had existed for a longer time prior to transition than the other cyclones in this study and, hence, its thermal field resembled that of a large occluded cyclone with the cyclone's SLP minimum far-removed from the peak of the thermal ridge. However, modest but localized frontogenesis did occur just to the west of the cyclone center. For Olga (Fig. 3d), strong frontogenesis was confined to the north of the PV maximum, which extended slightly to the west of the SLP minimum. Additionally, a warm anomaly coincident with the cyclone center had been enclosed almost entirely by cooler air bordering the southern half of the cyclone. Delta (Fig. 3e) was similar to Karen in that a lengthy band of frontogenesis extended from along the warm front to northwest of the SLP minimum on a bent-back front. However, Delta's thermal field resembled that of an occluded cyclone with the SLP minimum far to the west of the peak of the warm sector. Epsilon (Fig. 3f) had a strong band of frontogenesis extending northeastward from the SLP minimum while a robust PV maximum existed at the end of the front.

As shown in Fig. 3, near the time of transition of each cyclone, strong frontogenesis occurred to the northwest of a low-level PV maximum located near the end of each cyclone's warm front. These regions of frontogenesis were associated with the production of heavy precipitation (not shown) and considerable LHR. Following
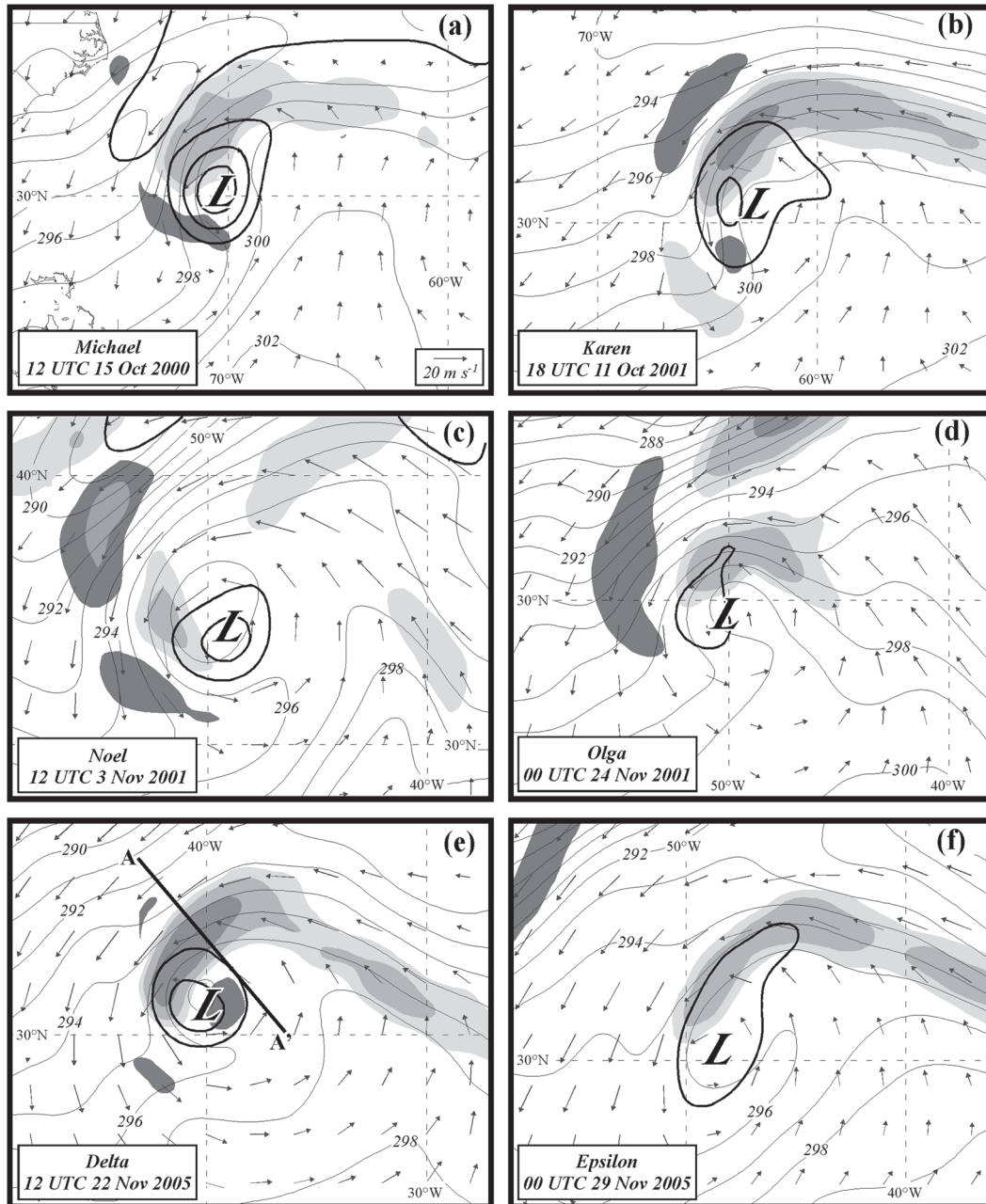
FIG. 3. FNL analyses of 850–950-hPa PV (thick black lines), 900-hPa potential temperature (thin gray lines), and 900-hPa frontogenesis (shaded) for (a) 1200 UTC 15 Oct 2000 (Michael), (b) 1800 UTC 11 Oct 2001 (Karen), (c) 1200 UTC 3 Nov 2001 (Noel), (d) 0000 UTC 24 Nov 2001 (Olga), (e) 1200 UTC 22 Nov 2005 (Delta), and (f) 0000 UTC 29 Nov 2005 (Epsilon). Temperature is labeled in K and contoured every 2 K. PV is labeled in PVU (1 PVU $\equiv$ 10^{-6} m^2 K kg^{-1} s^{-1}) and contoured every 0.25 PVU beginning at 0.5 PVU. Frontogenesis is contoured in frontogenesis units [FGU = K (100 km)$^{-1}$ (3 h)$^{-1}$] and is shaded every 0.2 FGU with light (dark) shading indicating positive (negative) frontogenesis. The "L" in (a)–(f) represents position of the SLP minimum.

the method employed by Emanuel et al. (1987), the rate of latent heating can be calculated as

$$H = \frac{d\theta}{dt} = \omega \left(\frac{\partial \theta}{\partial p} - \frac{\gamma_m}{\gamma_d} \frac{\theta}{\theta_e} \frac{\partial \theta_e}{\partial p} \right), \qquad (4)$$

where H corresponds to latent heat release, ω is the vertical velocity (in Pa s^{-1}), θ_e is the equivalent potential temperature, and γ_d and γ_m are the dry and moist adiabatic lapse rates, respectively. Quantitative values of PV generation in the lower troposphere are obtained by

inserting values of the calculated LHR into an explicit computation of the diabatic, nonadvective time tendency of PV. Following Cammas et al. (1994), the local nonadvective change in PV can be written as

$$\frac{\partial PV}{\partial t} = -g\mathbf{V}_p \cdot \mathbf{Y}, \tag{5}$$

where g is the gravitational acceleration, and $\mathbf{V}_p$ is the three-dimensional vector gradient ($\mathbf{V}_p = \partial/\partial x\mathbf{i} + \partial/\partial y\mathbf{j} - \partial/\partial p\mathbf{k}$). The nonadvective potential vorticity flux vector is

$$\mathbf{Y} = -H\boldsymbol{\zeta}_\alpha + \mathbf{V}_p\theta \times \mathbf{F}, \tag{6}$$

where $\boldsymbol{\zeta}_\alpha$ is the three-dimensional absolute vorticity vector ($\zeta_x = \partial v/\partial p, \zeta_y = -\partial u/\partial p, \zeta_p + f$) and $\mathbf{F}$ is the friction force. For the purposes of the present investigation, we neglect the effects of friction and focus solely on the time tendency of PV associated with LHR, which may be written as

$$\frac{\partial PV}{\partial t} = -g\mathbf{V}_p \cdot \mathbf{Y} = g\boldsymbol{\zeta}_\alpha \cdot \mathbf{V}_p H. \tag{7}$$

Figure 4 shows the low-level frontogenesis, PV, and the local nonadvective change in PV at 900 hPa for each storm at the same times as in Fig. 3. Note that in each case the nonadvective PV tendency is maximized to the west (northwest, west, or southwest) of the cyclone center. These nonadvective tendencies are, in each case, an order of magnitude larger than the horizontal PV advection at 900 hPa. To the extent that positive PV tendencies are associated with cyclonic development, such a distribution encourages a westward propagation of the cyclone center near the time of transition and suggests that this propagation is the by-product of LHR in convection located west of the cyclone center. Simultaneously, corresponding negative PV tendencies at upper-tropospheric levels in the same vertical columns (to be shown in Fig. 7) served to reduce the vertical shear in the columns toward which the cyclones were moving.

Prior to the transition of each cyclone, strong frontogenesis occurred to the northwest of a low-level PV maximum located at the end of each cyclone's bent-back warm front. For each case, the frontogenetical region was characterized by an area of confluence where winds having a cross-front component on the warm side of the front met with mostly front-parallel winds on the cool side of the front. Additionally, cooler air had begun to wrap around each cyclone in varying degrees by the times shown in Fig. 3, a trend that was encouraged to continue in each case as cold air advection was occurring

to the south of each cyclone. Strong winds, approaching 30 m s^{-1} in a few cases, existed on the cool side of the bent-back warm front in each case. As a consequence of their northerly direction, these winds likely exported cooler, drier air over the warm ocean thereby enhancing the transfer of sensible/latent heat from the ocean to the atmosphere and promoting destabilization. Additionally, each cyclone was in the process of moving westward during the period of intense frontogenesis (see Fig. 1).

Given their common configuration in all six cases, low-level PV and frontogenesis appear to be strongly interactive during tropical transition. In fact, the coincidence of large diabatic PV production by LHR and the maximum lower-tropospheric PV itself in each case is suggestive of a frontogenetically driven, diabatic origin for the low-level PV maxima in these cases of tropical transition. Figure 5 displays the 900-hPa frontogenesis and low-level PV fields over a portion of the life cycle of Michael. For ease of illustration, Fig. 6 includes the diabatic PV tendency due to LHR along with the low-level PV and frontogenesis over the same period of Michael's life cycle. The evolution observed here is representative of all six cases with regard to the general positions and trends of the frontogenesis, low-level PV maxima, and diabatic PV tendency. At 0000 UTC 14 October 2001 (36 h prior to tropical designation), a linear band of PV identified the stationary front along which Michael's precursor developed (Fig. 5a). Moderate frontogenesis was coincident with the area of enhanced PV near the newly formed SLP minimum. Robust diabatic PV tendency was associated with the updraft portion of the thermally direct circulation implied by the frontogenesis (Fig. 6a). The cyclone was further developed 18 h later with an ellipsoidal PV anomaly located at the intersection between the warm front extending northeastward and a cold front extending to the south (Fig. 5b). Intense frontogenesis, with a maximum value higher than observed at any other time during the transition, occurred directly to the north of the SLP minimum in an area of enhanced confluence at this time. The largest diabatic PV tendency was associated with this region of frontogenesis (Fig. 6b). By 1200 UTC 15 October, the strongest frontogenesis had rotated into the northwest quadrant of the cyclone and its intensity had slightly decreased (Fig. 5c). A strong, more circular PV anomaly became collocated with the SLP minimum with only a slight ridging of PV along the cyclone's warm front. The diabatic PV tendency maximum followed the frontogenesis to the northwest of the cyclone center by this time (Fig. 6c) and was a direct result of the intense convection in this region (see Fig. 2b of Davis and Bosart (2004)). By 0600 UTC 16 October the frontogenesis had almost entirely diminished (Fig. 5d) and the thermal field in the
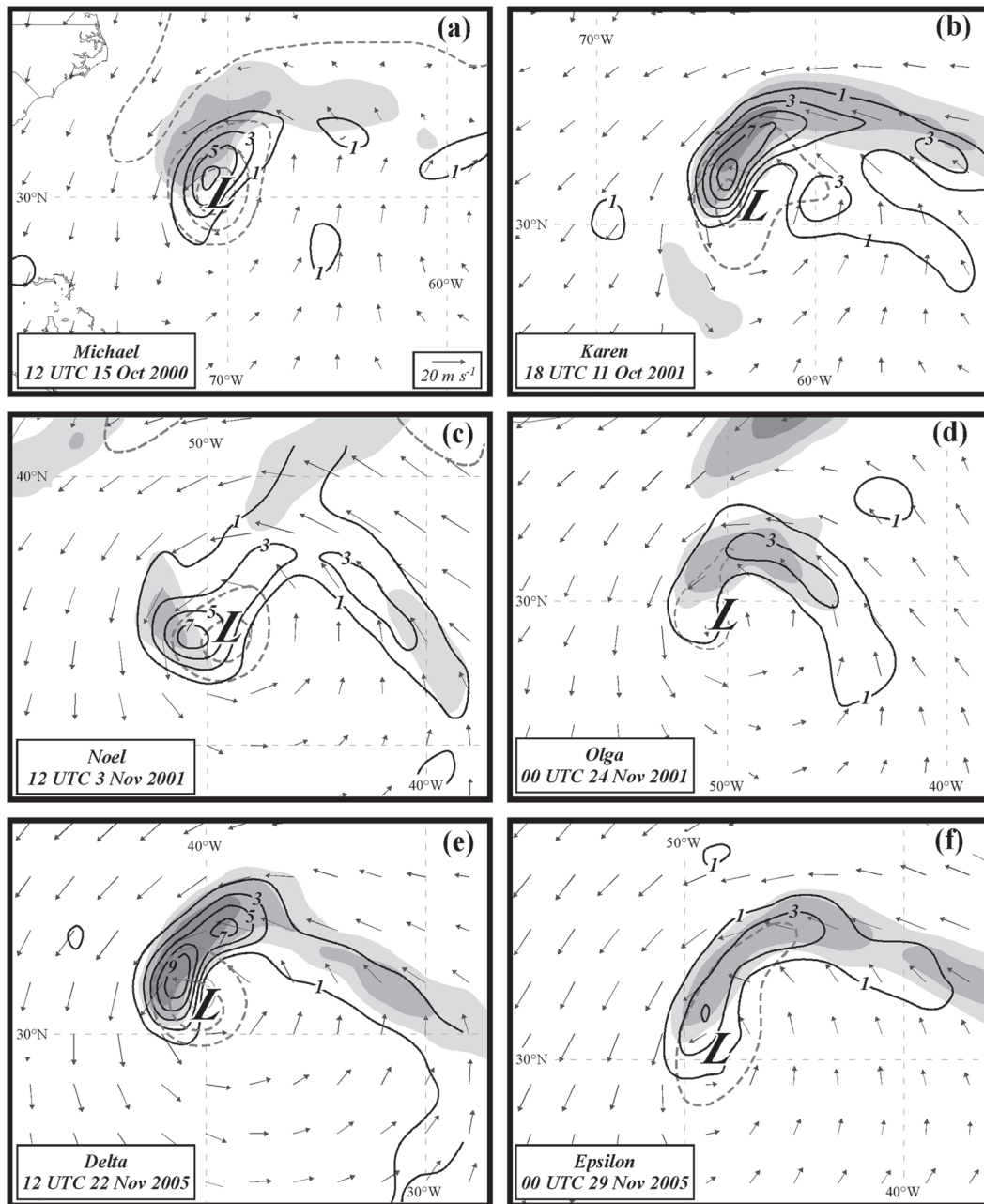
FIG. 4. As in Fig. 3, but FNL analyses of 900-hPa frontogenesis (shaded), 850–950-hPa PV (dashed gray lines), and 900-hPa diabatic PV tendency. Frontogenesis shaded as in Fig. 3 and PV labeled and contoured, though with dashed lines, as in Fig. 3. Diabatic PV tendency is labeled in PVU day^{-1} and contoured every 2 PVU day^{-1} beginning at 1 PVU day^{-1}.

vicinity of the cyclone had become more axisymmetric with a warm anomaly at the center and no sharp temperature gradients. Interestingly, the largest diabatic PV tendencies of the entire life cycle occurred coincident with the nearly circular low-level PV maximum indicating that the convective heating was no longer tied to lower-tropospheric frontogenesis by this time (Fig. 6d).

By 0000 UTC 17 October, the PV/wind fields were symmetric and no clear frontal structure existed in the near vicinity of the cyclone (Fig. 5e). The diabatic PV tendency near the cyclone center had also decreased by this time (Fig. 6e). Thus, for Michael, the area of frontogenesis rotated cyclonically around the cyclone center dragging the diabatic PV tendency maximum
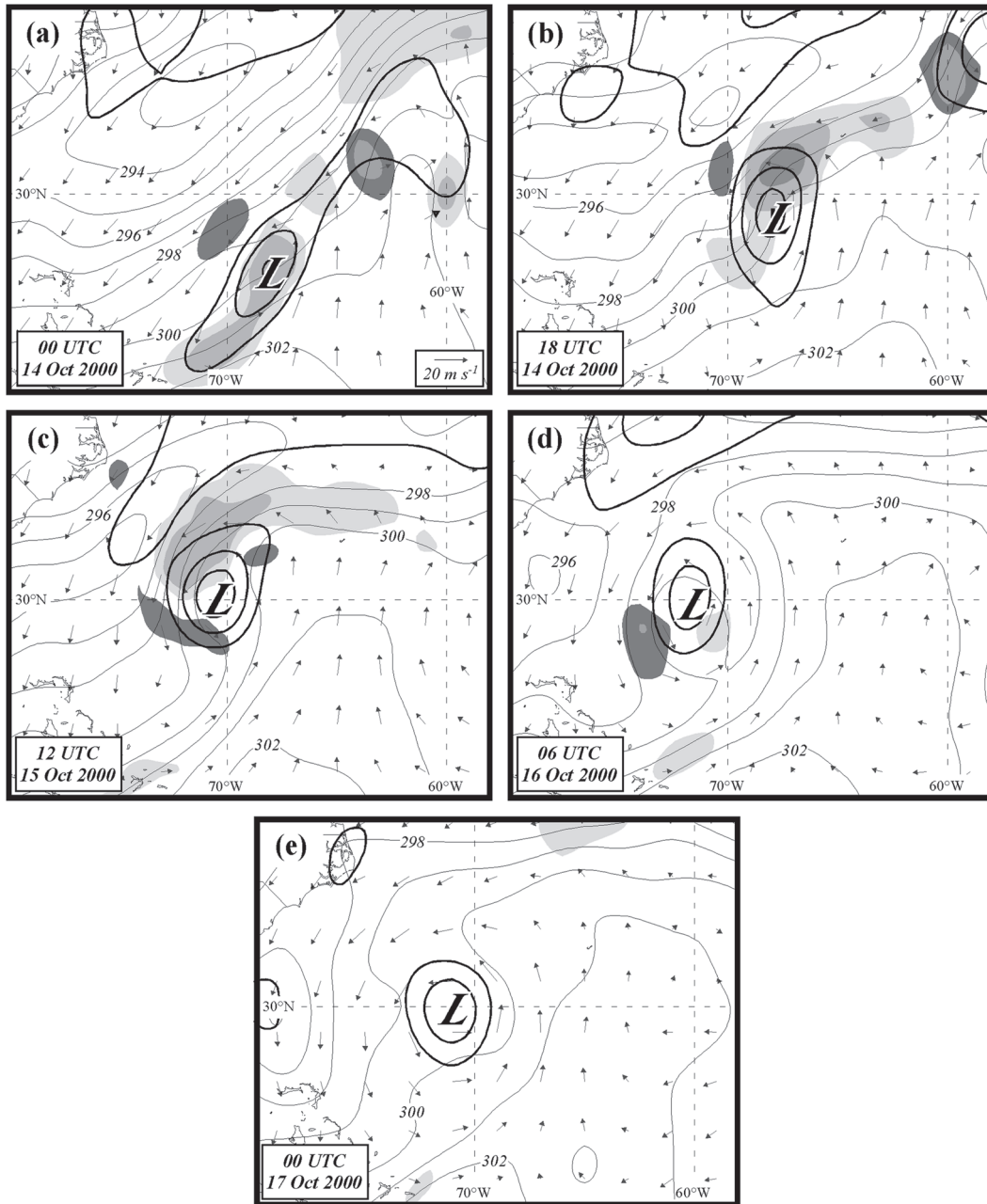
FIG. 5. As in Fig. 3, but for (a) 0000 UTC 14 Oct 2000, (b) 1800 UTC 14 Oct 2000, (c) 1200 UTC 15 Oct 2000, (d) 0600 UTC 16 Oct 2000, and (e) 0000 UTC 17 Oct 2000.

with it. At the same time, the PV itself became better organized at the terminus of the bent-back warm front. This set of circumstances served to displace the intensifying low-level circulation progressively farther west in the period preceding tropical transition.

b. Upper-level potential vorticity

In each of the six cases studied here, tropical transition was preceded by the migration of a distinct upper-level

PV anomaly from the midlatitudes into the subtropics where it was subsequently altered and weakened during the tropical transition process. Figure 7 shows the evolution of the upper-level PV field over Noel, which is representative of the PV evolution of all six cases. One day prior to tropical designation (1200 UTC 2 November 2001), a large-magnitude PV anomaly was located west of Noel's SLP minimum (Fig. 7a). By 0000 UTC 3 November, the upper-level PV feature had begun to
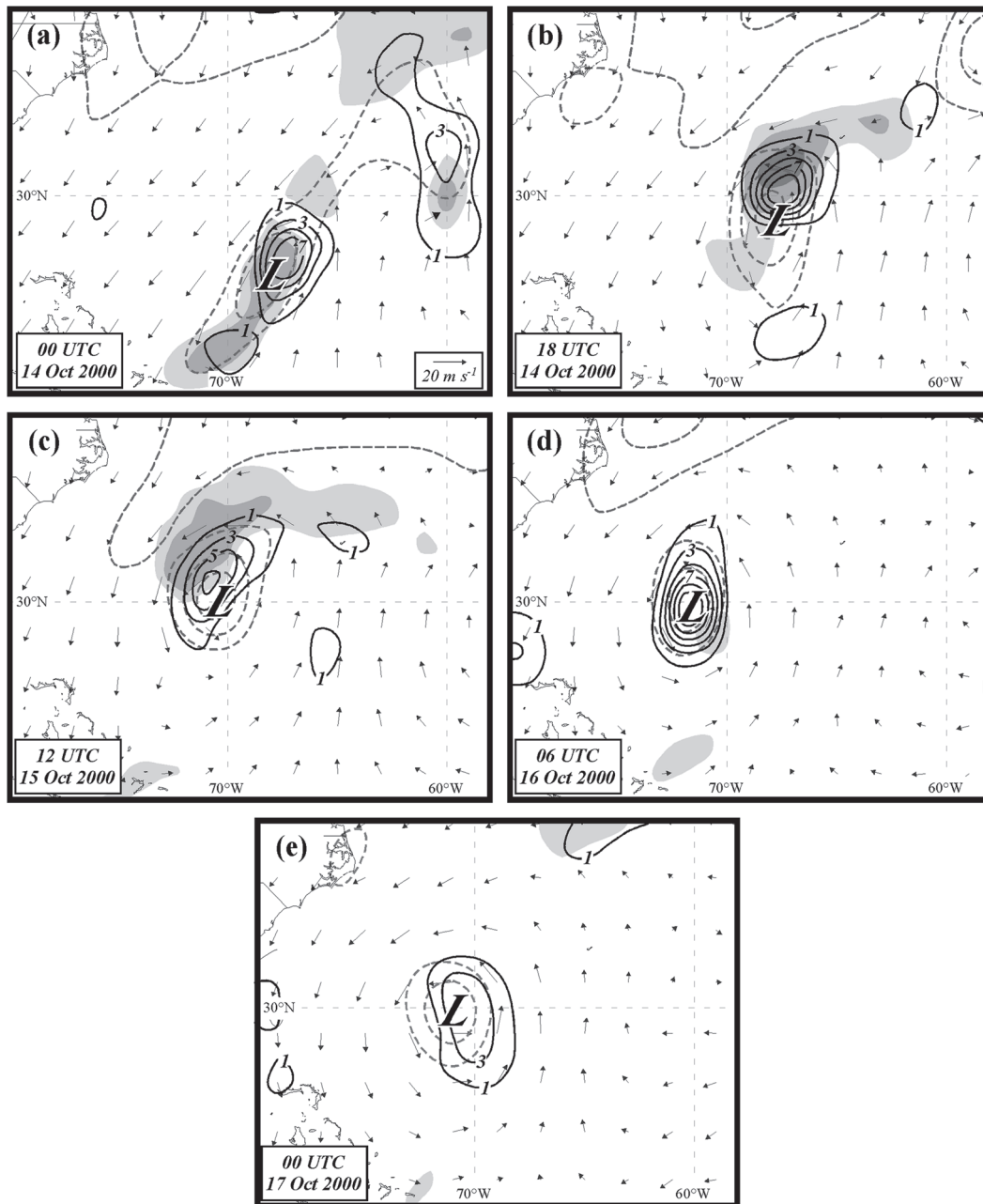
FIG. 6. As in Fig. 4, but for (a) 0000 UTC 14 Oct 2000, (b) 1800 UTC 14 Oct 2000, (c) 1200 UTC 15 Oct 2000, (d) 0600 UTC 16 Oct 2000, and (e) 0000 UTC 17 Oct 2000.

deform as high PV began wrapping around to the south of the cyclone and low PV air was streaming to the northwest (Fig. 7b). The ridging evident in the anticyclonic turning of the upper-level winds to the north of the cyclone center is consistent with the diabatic PV destruction and attendant ridge building that was occurring there. Additionally, the surface cyclone had moved to the west temporarily placing it under an area of stronger upper-level PV gradients. The deformation of

the upper-level PV field continued such that by 1200 UTC 3 November the anomaly began to detach from the midlatitude westerlies and the trough became cut off (Fig. 7c). Noel's center moved quickly to the west under the nose of the upper-level PV feature, which resembled the treble clef structure observed in occluded cyclones (Martin 1998). Strong PV gradients still existed over the eastern half of the cyclone; however, the area immediately west of the cyclone, in the direction the cyclone
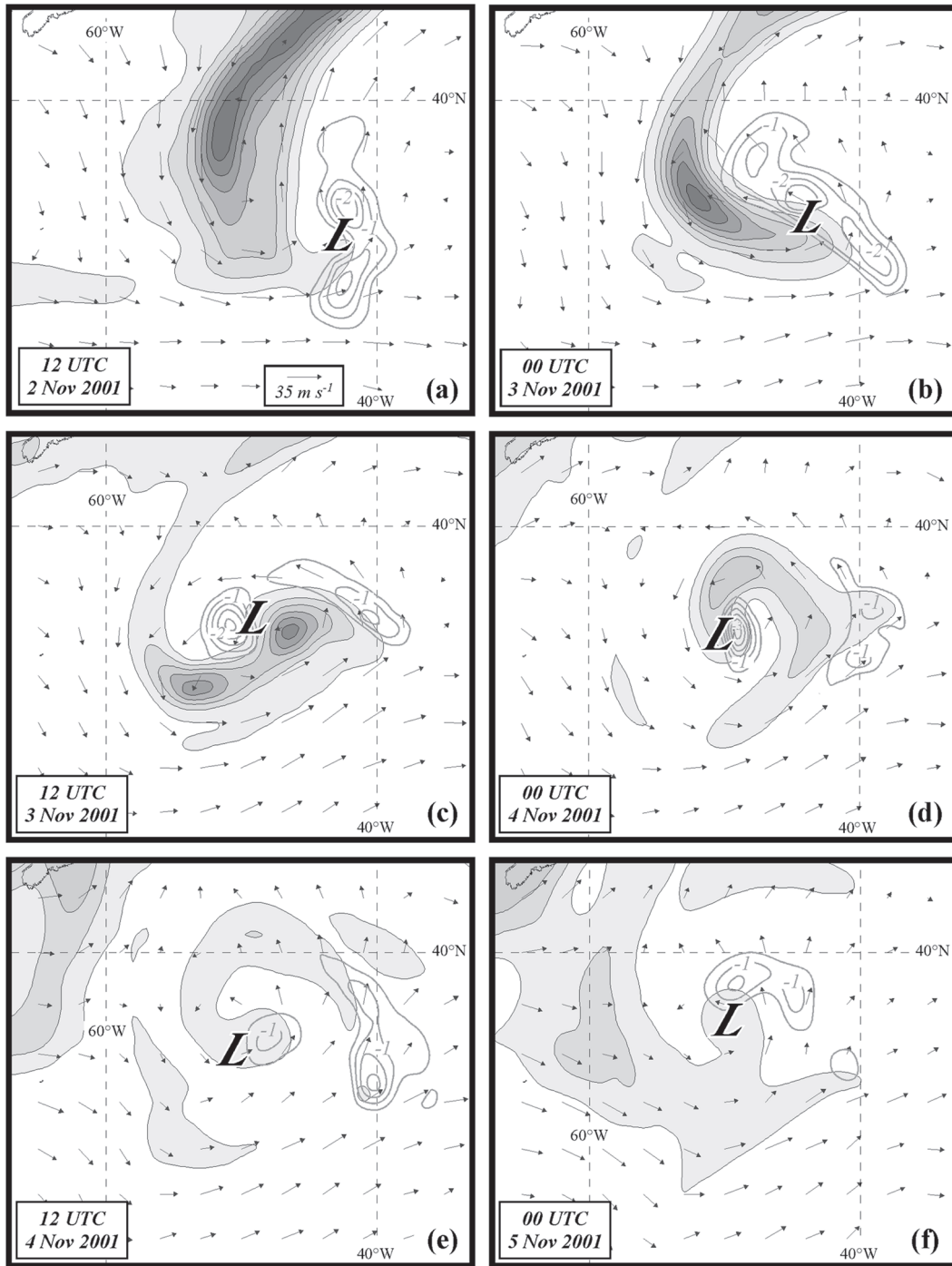
FIG. 7. FNL analyses of 325–335-K PV (PVU, filled), 330-K winds (arrows), and 330-K diabatic PV tendency (gray lines) for (a) 1200 UTC 2 Nov 2001, (b) 0000 UTC 3 Nov 2001, (c) 1200 UTC 3 Nov 2001, (d) 0000 UTC 4 Nov 2001, (e) 1200 UTC 4 Nov 2001, and (f) 0000 UTC 5 Nov 2001. PV contoured and shaded every 1 PVU beginning at 1 PVU. Diabatic PV tendency labeled in PVU day^{-1} and contoured every 0.5 PVU day^{-1} beginning at -0.5 PVU day^{-1}. The "L" in (a)–f) represents position of the SLP minimum.

was moving, contained weak PV gradients and, consequently, small vertical shear. The upper-level PV feature was completely isolated by 0000 UTC 4 November (Fig. 7d). As Noel continued to develop tropical characteristics, the upper-level PV feature continued to weaken (Fig. 7e). By 0000 UTC 5 November the upper-level PV feature had nearly disappeared and the PV gradient over Noel was near zero (Fig. 7f). Accordingly, vertical shear over the cyclone was small (10.5 m s^{-1}) and the cyclone was able to reach hurricane status during the day on 5 November. It is interesting to note that according to the HURDAT data, Noel had reached a minimum SLP of 988 hPa by 0000 UTC 4 November at the end of the period in which strong PV gradients/vertical shear influenced the cyclone. Noel's minimum value of SLP actually increased on 4 November when the upper-level PV feature was weakening and the cyclone did not start to deepen again until just before reaching hurricane status. This period of quiescence is reminiscent of the simulation of Michael reported by Davis and Bosart (2003).

Around the time of tropical designation, the upper-level PV field over each cyclone resembled the treble clef structure with anomalously high (low) PV air to the south (north) of the SLP minimum (Fig. 8). Also at the times pictured, each cyclone sat beneath a column capped with large PV gradients. However, every cyclone was moving westward (except Olga, which was moving eastward yet decreasing in forward speed) on trajectories that were systematically acting to place each cyclone under an area of weaker upper-level PV gradients and, hence, smaller vertical shear.

c. Upshear convection

Around the time of intense frontogenesis and the first appearance of a treble clef in the upper-level PV field, each cyclone appeared to develop robust convection on its western/southwestern side as suggested by the IR satellite imagery displayed in Fig. 9.[7] The collocation of the convection and frontogenesis warrants an analysis of the vertical structure in the vicinity of the front. Figure 10 shows a vertical cross section, characteristic of all six cases near or just prior to transition, taken perpendicular to the bent-back front and through the area of maximum vertical motion associated with Delta. Above 750 hPa, the thermal structure strongly resembled that of the canonical warm occlusion with an axis of maximum θ_e tilting poleward and westward with height sep-

arating cold and warm frontal zones manifest as gradients of θ_e (Fig. 10a).[8] The resemblance to an occluded thermal structure was absent near the surface because of the presence of a moist, convectively unstable boundary layer and a slanted column of moist air to the west (upshear) of the cyclone. The upshear moist axis tilted over strong low-level winds to the north of the warm front and extended upward from an area of boundary layer convergence (not shown).

Figure 10b illustrates the connection between the frontogenesis and its associated deep vertical circulation. The tilted region of maximum ascent along the warm edge of the warm frontal zone (from ~850 to 650 hPa) occurs in an environment of nearly constant θ_e shown in Fig. 10a. Additionally, the area of maximum updraft appeared to connect the most unstable portion of the boundary layer with the axis of maximum θ_e associated with the warm-occluded structure aloft.

By the end of the period of intense frontogenesis and upper-level PV deformation and destruction, each cyclone sat beneath the center of an upper-level trough or cutoff (Fig. 11). The baroclinicity that existed at the time of cyclogenesis had disappeared and been replaced by a more uniform and, in some cases (Karen; Fig. 11b), axisymmetric temperature field. With upper-level winds over each cyclone less than 15 m s^{-1} (Table 2), vertical shear was low enough to allow each cyclone to develop and maintain tropical characteristics. After this point, each cyclone evolved uniquely based on differing environmental conditions that influenced its strength and movement. Michael, Karen, and Noel moved northward and underwent extratropical transition. Olga meandered to the west and persisted for two weeks. Moving eastward, Delta impacted Africa as an extratropical cyclone and Epsilon decayed in the eastern Atlantic after 10 days as a tropical cyclone.

4. Summary and discussion

Tropical transition is the process by which a vertically sheared, extratropical cyclone powered by baroclinic conversion is transformed into a warm-core, vertically stacked tropical cyclone capable of amplifying by air–sea interaction processes [i.e., wind-induced surface heat exchange (WISHE) Emanuel (1986)]. Recent work by Davis and Bosart (2003, 2004) has identified a number of salient characteristics of such events. In this paper, six recent cases of SEC tropical transition in the Atlantic basin have been compared in order to better understand

---

[7] Numerical simulations of a subset of these cases (not shown) confirm the reasonable suspicion that such IR signatures are nearly certain proxies for the occurrence of robust convection.

[8] The baroclinicity associated with the cold and warm fronts, though meager, is illustrated in the cross-section of potential temperature in Fig. 10b.
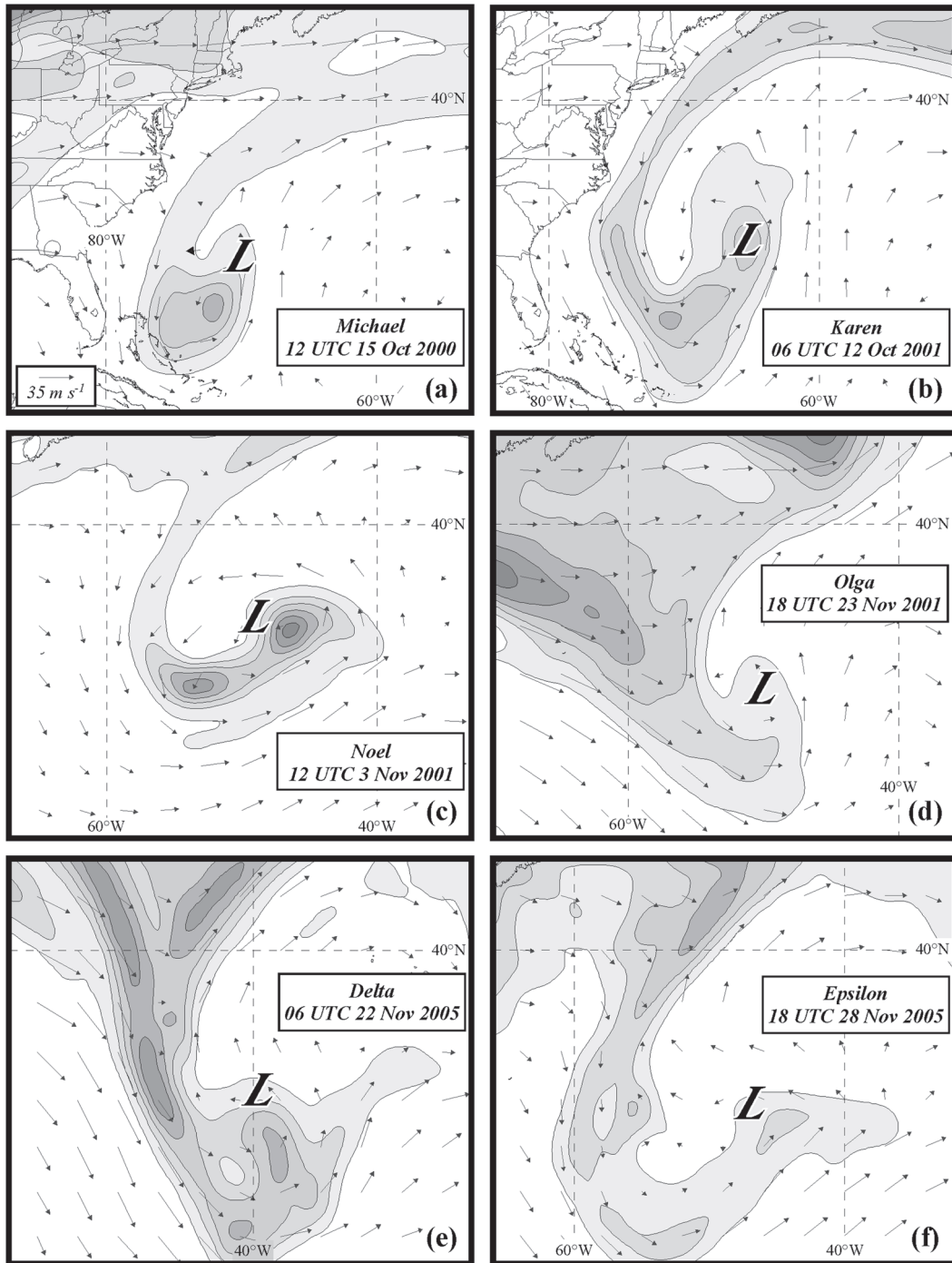
FIG. 8. FNL analyses of (a) 335–345-K PV (PVU, filled) and 340-K winds (arrows) for 1200 UTC 15 Oct 2000 (Michael), (b) 335–345-K PV and 340-K winds for 0600 UTC 12 Oct 2001 (Karen), (c) 325–335-K PV and 330-K winds for 1200 UTC 3 Nov 2001 (Noel), (d) 330–340-K PV and 335-K winds for 1800 UTC 23 Nov 2001 (Olga), (e) 330–340-K PV and 335-K winds for 0600 UTC 22 Nov 2005 (Delta), and (f) 325–335-K PV and 330-K winds for 1800 UTC 28 Nov 2005 (Epsilon). PV contoured and shaded as in Fig. 7. The "L" in (a)–(f) represents position of the SLP minimum.
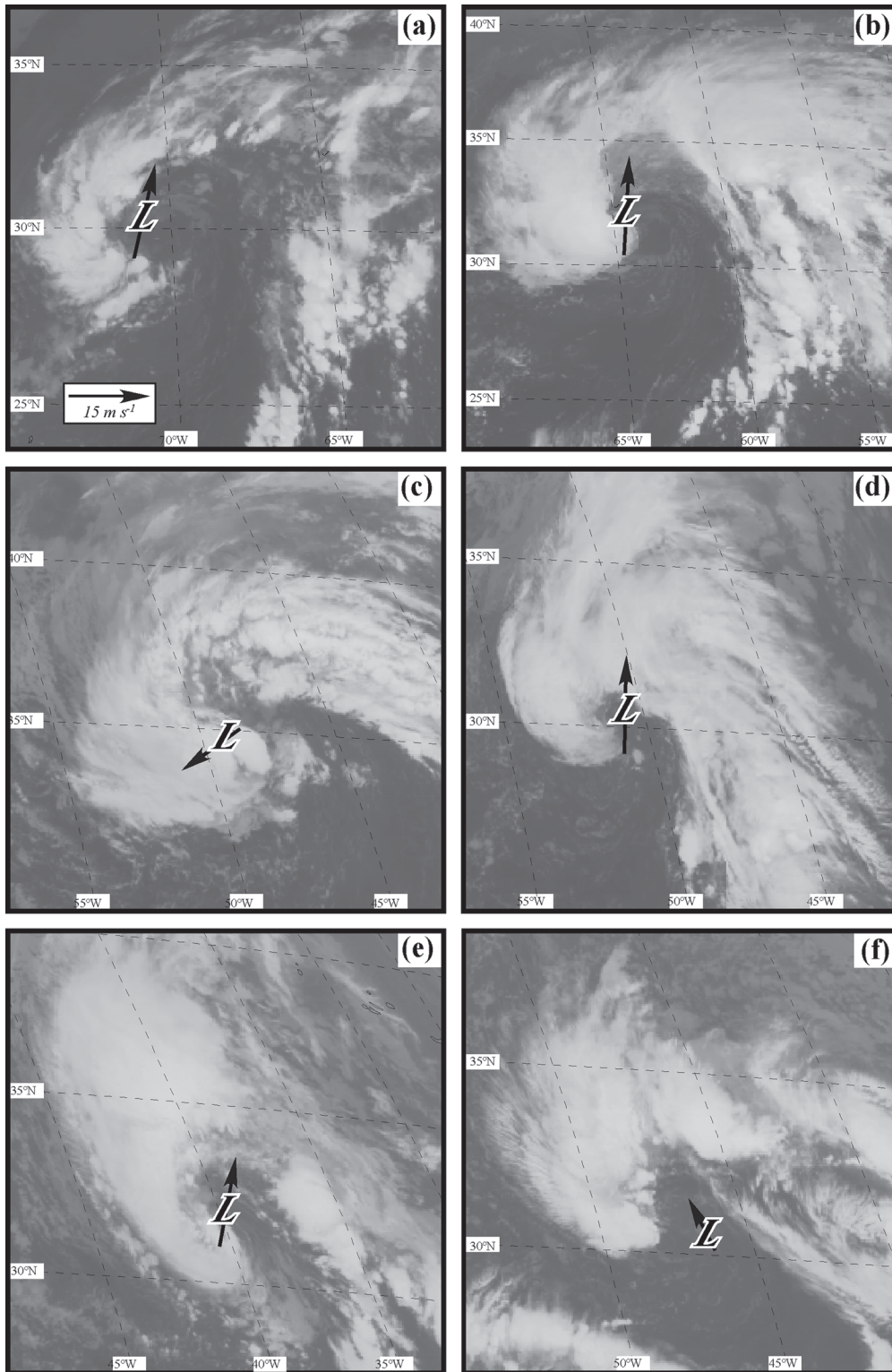
FIG. 9. Infrared satellite images from (a) 1115 UTC 15 Oct 2000 (Michael), (b) 2215 UTC 11 Oct 2001 (Karen), (c) 0915 UTC 3 Nov 2001 (Noel), (d) 0815 UTC 23 Nov 2001 (Olga), (e) 0415 UTC 22 Nov 2005 (Delta), and (f) 1115 UTC 28 Nov 2005 (Epsilon). Thick black arrow in (a)–(f) indicates the direction and magnitude of the 200–900-hPa vertical shear over the cyclone center determined as in Table 2.
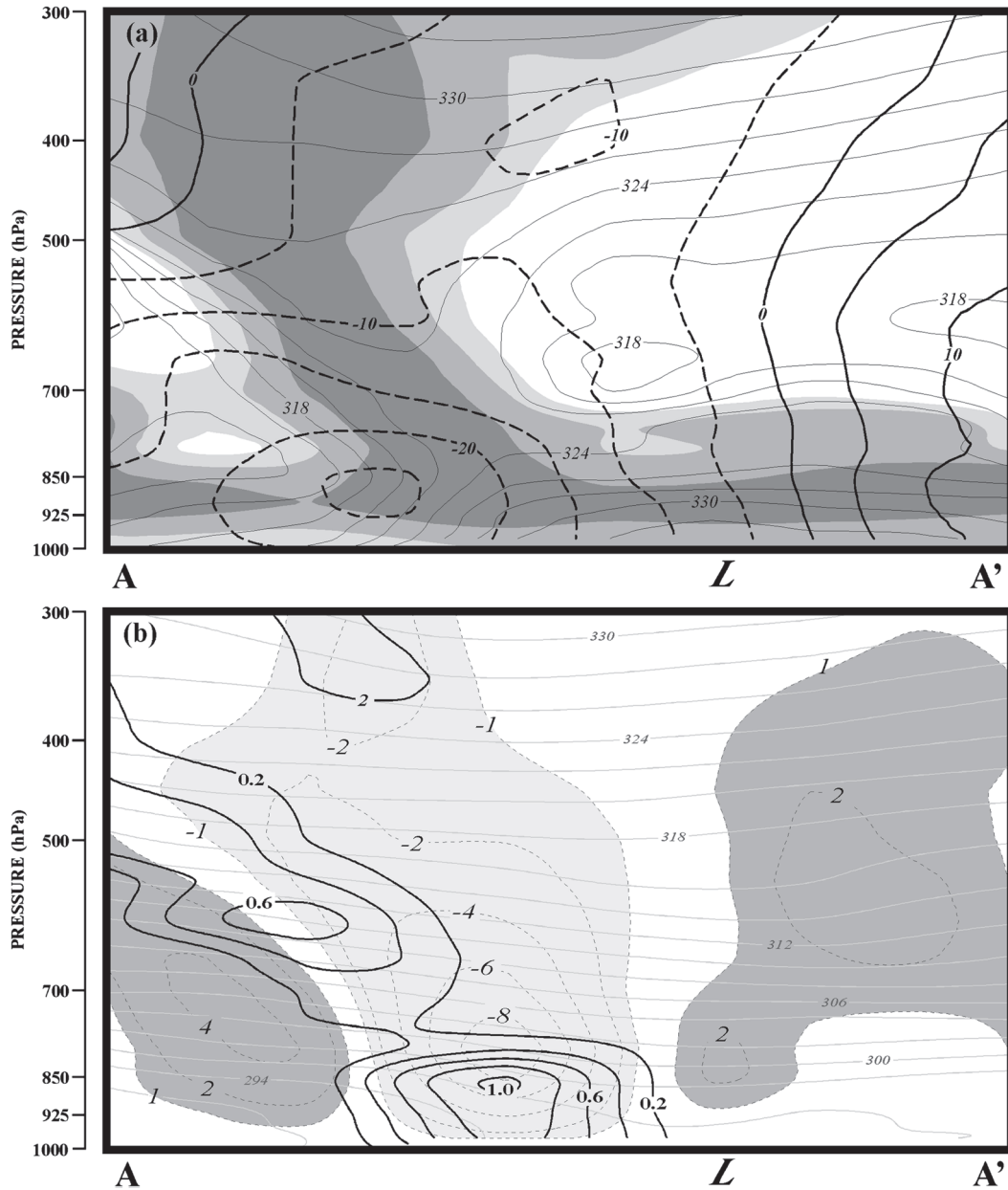
FIG. 10. Cross section, along A–A′ in Fig. 3e, from the FNL analysis at 1200 UTC 22 Nov 2005. (a) Thick lines are contours of wind speed normal to the cross section (m s^{-1}, values hatched coming out of the page), thin lines are contours of equivalent potential temperature (θ_e, K), and shaded areas represent relative humidity. (b) Thin gray lines are isentropes labeled in K and contoured every 2 K. Thick black lines are positive frontotgenesis labeled in FGU and contoured every 0.2 FGU beginning at 0.2 FGU. Thin dashed lines are ω, labeled in dPa s^{-1} and contoured every -2 (2) dPa s^{-1} beginning at -2 (2) dPa s^{-1} and also including -1 (1) dPa s^{-1} contour, with light (dark) shading indicating region of ascent (descent). The "L" on the cross section represents the position of the SLP minimum.

the manner by which some of the canonical structures and dynamical processes of extratropical cyclones become involved in preconditioning the precursor cyclone for transition.

In each case examined here, as in the transition events described in Davis and Bosart (2003), the precursor

extratropical cyclone developed in an environment characterized by vertical shear large enough to effectively prohibit tropical cyclone formation from tropical waves. Initial development of the precursor ensued as an upper-tropospheric shortwave trough encroached upon a low-level baroclinic zone (Petterssen and Smebye
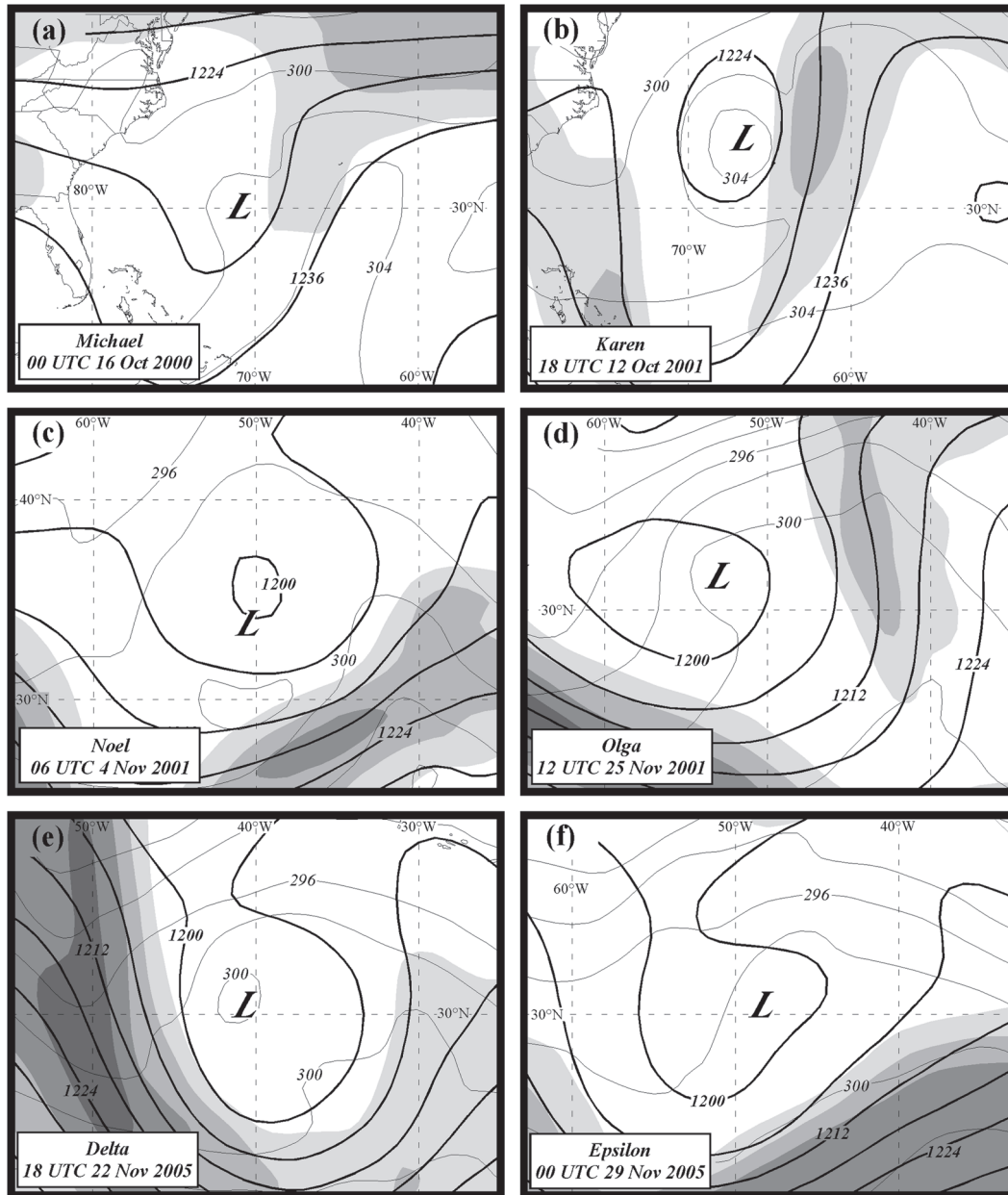
FIG. 11. As in Fig. 2, but for (a) 0000 UTC 16 Oct 2000 (Michael), (b) 1800 UTC 12 Oct 2001 (Karen), (c) 0600 UTC 4 Nov 2001 (Noel), (d) 1200 UTC 25 Nov 2001 (Olga), (e) 1800 UTC 22 Nov 2005 (Delta), and (f) 0000 UTC 29 Nov 2005 (Epsilon).

1971). This circumstance promotes upward vertical motion via cyclonic vorticity advection by the thermal wind (Sutcliffe 1947; Trenberth 1978) and distorts the linear baroclinic zone into a frontal wave (Martin 2006). Eventually, a closed circulation and sea level pressure minimum form at the surface. Along the nascent cyclone's frontal zones, precipitation develops in linear bands in response to frontogenesis that tends to be more intense along the warm front which, in subtropical cy-

clones, is usually more baroclinic. As it continues to mature, the SEC precursor eventually exhibits a bent-back warm/occluded front extending into the cool air west and northwest of the surface cyclone center similar to phase 3 of the Shapiro and Keyser (1990) conceptual model of marine extratropical cyclones. In all six cases, an area of frontogenesis characterizes this front, first intensifying and then weakening as the cyclone approaches transition. Within the resultant circulation,
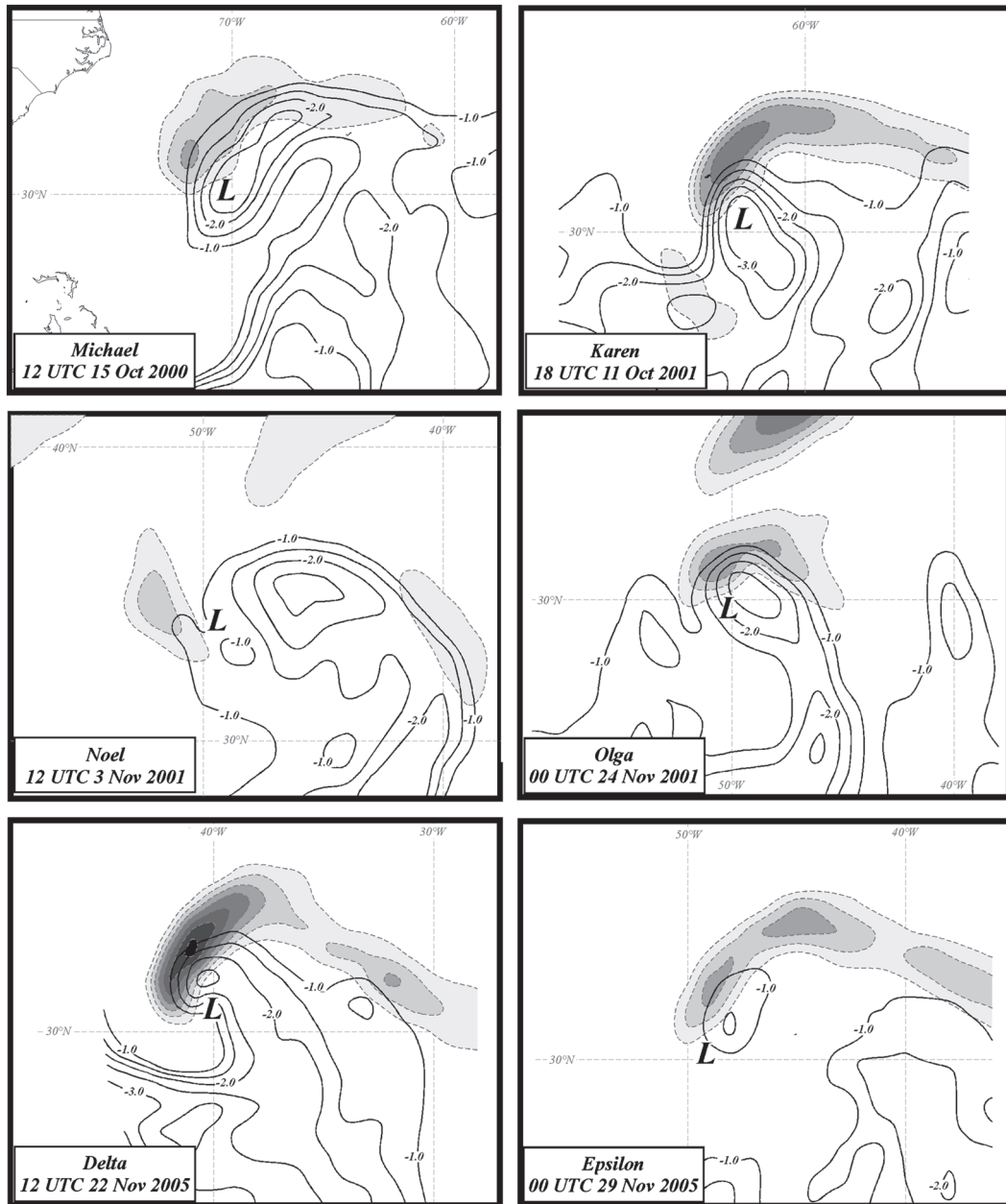
FIG. 12. FNL analyses of 900-hPa positive frontogenesis (dashed lines with shading) and negative 900–500-hPa θ_e lapse rate (solid lines) for (a) 1200 UTC 15 Oct 2000 (Michael), (b) 1800 UTC 11 Oct 2001 (Karen), (c) 1200 UTC 3 Nov 2001 (Noel), (d) 0000 UTC 24 Nov 2001 (Olga), (e) 1200 UTC 22 Nov 2005 (Delta), and (f) 0000 UTC 29 Nov 2005 (Epsilon). Frontogenesis labeled, contoured, and shaded as in Fig. 3. The 500–900-hPa θ_e lapse rate is labeled in K km^{-1} and contoured every -0.5 K km^{-1} beginning at -0.5 K km^{-1}. The "L" in (a)–(f) represents the position on the SLP minimum.

precipitation develops and, via diabatic redistribution of PV, promotes the growth of a low-level PV strip along the warm front.

As this lower-tropospheric PV anomaly grows via persistent latent heat release, and accumulates at the end of the front, the low-level circulation around the cyclone center also intensifies. Since the low-level flow on the cold side of the bent-back front is northerly or northeasterly and the upper-level flow is southwesterly downstream of the upper trough axis, the northwest quadrant of the storm is characterized by large southwesterly vertical shear. This circumstance results in two

important, interrelated structural features of the occluding cyclone. First, the large vertical shear in the northwest quadrant coupled with the nearly moist neutral occluded thermal structure above the boundary layer, renders the effective static stability very low in the occluded quadrant. Second, the superposition of strong lower-tropospheric frontogenesis with minimal resistance to vertical displacement in the northwest quadrant of the storm (Fig. 12) promotes the convective burst that characterizes each transition event. The resulting convective heating reduces the upper-tropospheric PV north and northwest of the surface cyclone while increasing it in the boundary layer near the surface cyclone. Such a diabatic rearrangement simultaneously strengthens the surface circulation while eroding upper-tropospheric PV and PV gradients just west of the surface cyclone center.

The prevelance of upshear convection at the time of occlusion was noted by Davis and Bosart (2004) as a characteristic of transition events. They point to the speed of occlusion as a key factor in whether or not a storm will undergo transition and argue that the necessary alacrity is provided by diabatic heating and its associated secondary circulation suggesting that extratropical occlusion *accelerated by diabatic heating* can lead to tropical transition. Posselt and Martin (2004) showed that diabatic heating is also of fundamental importance to the midlatitude occlusion process. They examined the effect of latent heat release on the development of an occluded thermal structure in a robust winter storm by comparing companion full physics and no-latent-heat-release simulations of the event performed using the MM5. They identified an adiabatic, synoptic-scale tendency for occlusion that operates too slowly to reproduce the structures observed in nature. Thus, the results offered here suggest that the "rapid occlusion" reported by Davis and Bosart (2003) as critical for tropical transition events is a manifestation of the inherently diabatic process of occlusion occurring at subtropical latitudes.

The survey presented here has pointed to the importance of frontal structure, frontal dynamics, and an updated view of the occlusion process in tropical transition events. Several similarities in the six cases appear to be the result of convection and its organization by, and interaction with, synoptic-scale features. The relatively coarse nature of the FNL dataset does not allow for explicit analysis of the convection and its feedback onto larger-scale flows during tropical transition. To elucidate the details of the interactions between convection and synoptic-scale processes suggested in this study, a companion paper will focus on a finescale simulation of a particular case of tropical transition. The

analysis of that simulation will provide the foundation for an improved conceptual model of tropical transition.

REFERENCES

Beven, J. L., S. R. Stewart, M. B. Lawrence, L. A. Avila, J. L. Franklin, and R. J. Pasch, 2003: Atlantic hurricane season of 2001. *Mon. Wea. Rev.,* **131,** 1454–1484.

——, and Coauthors, 2008: Atlantic hurricane season of 2005. *Mon. Wea. Rev.,* **136,** 1109–1173.

Bosart, L. F., 1981: The Presidents' Day Snowstorm of 18–19 February 1979: A sub-synoptic scale event. *Mon. Wea. Rev.,* **109,** 1542–1566.

Bracken, W. E., and L. F. Bosart, 2000: The role of synoptic-scale flow during tropical cyclogenesis over the North Atlantic Ocean. *Mon. Wea. Rev.,* **128,** 353–376.

Cammas, J.-P., D. Keyser, G. M. Lackmann, and J. Molinari, 1994: Diabatic redistribution of potential vorticity accompanying the development of an outflow jet within a strong extratropical cyclone. Preprints, *Int. Symp. on the Life Cycles of Extratropical Cyclones,* Vol. II, Bergen, Norway, Geophysical Institute, University of Bergen, 403–409.

Davis, C. A., and L. F. Bosart, 2003: Baroclinically induced tropical cyclogenesis. *Mon. Wea. Rev.,* **131,** 2730–2747.

——, and ——, 2004: The TT problem: Forecasting the tropical transition of cyclones. *Bull. Amer. Meteor. Soc.,* **85,** 1657–1662.

DeMaria, M., J. A. Knaff, and B. H. Connell, 2001: A tropical cyclone genesis parameter for the tropical Atlantic. *Wea. Forecasting,* **16,** 219–233.

Emanuel, K. A., 1986: An air-sea interaction theory for tropical cyclones. Part I: Steady-state maintainence. *J. Atmos. Sci.,* **43,** 585–605.

——, M. Fantini, and A. J. Thorpe, 1987: Baroclinic instability in an environment of small stability to slantwise moist convection. Part I: Two-dimensional models. *J. Atmos. Sci.,* **44,** 1559–1573.

Foley, G. R., and B. N. Hanstrum, 1994: The capture of tropical cyclones by cold fronts off the west coast of Australia. *Wea. Forecasting,* **9,** 577–592.

Franklin, J. L., L. A. Avila, J. L. Beven, M. B. Lawrence, R. J. Pasch, and S. R. Stewart, 2001: Atlantic hurricane season of 2000. *Mon. Wea. Rev.,* **129,** 3037–3056.

Hanley, D., J. Molinari, and D. Keyser, 2001: A composite study of the interactions between tropical cyclones and upper-tropospheric troughs. *Mon. Wea. Rev.,* **129,** 2570–2584.

Harr, P. A., and R. L. Elsberry, 2000: Extratropical transition of tropical cyclones over the western North Pacific. Part I: Evolution of structural characteristics during the transition process. *Mon. Wea. Rev.,* **128,** 2613–2633.

Hart, R. E., 2003: A cyclone phase space derived from thermal wind thermal asymmetry. *Mon. Wea. Rev.,* **131,** 585–616.

——, and J. L. Evans, 2001: A climatology of the extratropical transition of Atlantic tropical cyclones. *J. Climate,* **14,** 546–564.

——, ——, and C. Evans, 2006: Synoptic composites of the extratropical transition life cycle of North Atlantic tropical cy-

clones: Factors determining posttransition evolution. *Mon. Wea. Rev.,* **134,** 553–578.

Hoskins, B. J., M. E. McIntyre, and A. W. Robertson, 1985: On the use and significance of isentropic potential vorticity maps. *Quart. J. Roy. Meteor. Soc.,* **111,** 877–946.

Hulme, A. L., and J. E. Martin, 2009: Synoptic- and frontal-scale influences on tropical transition events in the Atlantic basin. Part II: Tropical transition of Hurricane Karen. *Mon. Wea. Rev.,* **137,** 3626–3650.

Jones, S. C., and Coauthors, 2003: The extratropical transition of tropical cyclones: Forecast challenges, current understanding, and future directions. *Wea. Forecasting,* **18,** 1052–1092.

Klein, P. M., P. A. Harr, and R. L. Elsberry, 2000: Extratropical transition of western North Pacific tropical cyclones: An overview and conceptual model of the transformation stage. *Wea. Forecasting,* **15,** 373–396.

Martin, J. E., 1998: The structure and evolution of a continental winter cyclone. Part I: Frontal structure and the classical occlusion process. *Mon. Wea. Rev.,* **126,** 303–328.

——, 2006: The role of shearwise and transverse quasigeostrophic vertical motions in the midlatitude cyclone life cycle. *Mon. Wea. Rev.,* **134,** 1174–1193.

McTaggart-Cowan, R., E. H. Atallah, J. R. Gyakum, and L. F. Bosart, 2006: Hurricane Juan (2003). Part I: A diagnostic and compositing life cycle study. *Mon. Wea. Rev.,* **134,** 1725–1747.

——, G. D. Dean, L. F. Bosart, C. A. Davis, and T. J. Galarneau, 2008: Climatology of tropical cyclogenesis in the North Atlantic (1948–2004). *Mon. Wea. Rev.,* **136,** 1284–1304.

Molinari, J., D. Vollaro, and K. L. Corbosiero, 2004: Tropical cyclone formation in a sheared environment: A case study. *J. Atmos. Sci.,* **61,** 2493–2509.

Montgomery, M. T., and B. F. Farrell, 1992: Polar low dynamics. *J. Atmos. Sci.,* **49,** 2484–2505.

Moore, R. W., and T. H. Vonder Haar, 2003: Diagnosis of a polar low warm core utilizing the Advanced Microwave Sounding Unit. *Wea. Forecasting,* **18,** 700–711.

Palmén, E., and C. W. Newton, 1969: *Atmospheric Circulation Systems: Their Structure and Physical Interpretation.* Academic Press, 603 pp.

Petterssen, S., and S. J. Smebye, 1971: On the development of extratropical cyclones. *Quart. J. Roy. Meteor. Soc.,* **97,** 457–482.

Posselt, D. J., and J. E. Martin, 2004: The effect of latent heat release on the evolution of a warm occluded thermal structure. *Mon. Wea. Rev.,* **132,** 578–599.

Rasmussen, E., 1981: An investigation of a polar low with a spiral cloud structure. *J. Atmos. Sci.,* **38,** 1785–1792.

Raymond, D. J., 1992: Nonlinear balance and potential vorticity thinking at large Rossby number. *Quart. J. Roy. Meteor. Soc.,* **118,** 987–1015.

Reale, O., and R. Atlas, 2001: Tropical cyclone–like vortices in the extratropics: Observational evidence and synoptic analysis. *Wea. Forecasting,* **16,** 7–34.

Reed, R. J., and M. D. Albright, 1986: A case study of explosive cyclogenesis in the Eastern Pacific. *Mon. Wea. Rev.,* **114,** 2297–2319.

Ritchie, E. A., and R. L. Elsberry, 2001: Simulations of the transformation stage of the extratropical transition of tropical cyclones. *Mon. Wea. Rev.,* **129,** 1462–1480.

Schär, C., and H. Wernli, 1993: Structure and evolution of an isolated semi-geostrophic cyclone. *Quart. J. Roy. Meteor. Soc.,* **119,** 57–90.

Shapiro, M. A., and D. Keyser, 1990: Fronts, jets streams, and the tropopause. *Extratropical Cyclones: The Erik Palmén Memorial Volume,* C. W. Newton and E. Holopainen, Eds., Amer. Meteor. Soc., 167–191.

Sinclair, M. R., 2002: Extratropical transition of southwest Pacific tropical cyclones. Part I: Climatology and mean structure changes. *Mon. Wea. Rev.,* **130,** 590–609.

Sousounis, P. J., J. Wallman, G. E. Mann, and T. J. Miner, 2001: ''Hurricane Huron'': An example of an extreme lake-aggregate effect in autumn. *Mon. Wea. Rev.,* **129,** 401–419.

Sutcliffe, R. C., 1947: A contribution to the problem of development. *Quart. J. Roy. Meteor. Soc.,* **73,** 370–383.

Takayabu, I., 1986: Roles of the horizontal advection on the formation of surface fronts and on occlusion of a cyclone developing in the baroclinic westerly jet. *J. Meteor. Soc. Japan,* **64,** 329–345.

Trenberth, K. E., 1978: On the interpretation of the diagnostic quasi-geostrophic omega equation. *Mon. Wea. Rev.,* **106,** 131–137.

Xu, Q., 1990: Cold and warm frontal circulations in an idealized moist semi-geostrophic baroclinic wave. *J. Atmos. Sci.,* **47,** 2337–2352.